# Synthesis and Characterization of Prussian Blue Modified Magnetite

**DATASET** · JANUARY 2013

READS
144

**5 AUTHORS**, INCLUDING:

Qian li Zhang
University of Leeds
**26** PUBLICATIONS **348** CITATIONS

SEE PROFILE

# Synthesis and Characterization of Prussian Blue Modified Magnetite Nanoparticles and Its Application to the Electrocatalytic Reduction of $H_2O_2$

Ge Zhao, Jiu-Ju Feng, Qian-Li Zhang, Shu-Ping Li, and Hong-Yuan Chen*

*Lab of Analytical Chemistry for Life Science (Education Ministry of China), Department of Chemistry, Nanjing University, Nanjing 210093, People's Republic of China*

*Received November 2, 2004. Revised Manuscript Received January 25, 2005*

Magnetite ($Fe_3O_4$) nanoparticles modified with electroactive Prussian Blue (PB) were first synthesized by a simple chemical method. Transmission electronic microscopy showed that the average size of the sample was about 12 nm, and X-ray powder diffraction, X-ray photoelectron spectroscopy, Fourier-transform IR, and UV−vis spectra showed the spinel structure for the nanoparticles and confirmed the existence of PB on the surface of $Fe_3O_4$. Magnetic properties of the sample were investigated by low-field alternating current susceptibility and superconducting quantum interference device measurement; the results indicated that the superparamagnetic properties remain for the sample with almost immeasurable remanence and coercivity at room temperature, while the value of saturation magnetization (Ms) reduces, and the blocking temperature ($T_B$) of PB modified $Fe_3O_4$ is around 150 K, lower than that of the pure $Fe_3O_4$ nanoparticles, so the interaction between the particles is decreased. More interesting, when at 5 K, the Ms of PB-modified $Fe_3O_4$ is greatly larger than that at 300 K and shows ferromagnetic behavior. Furthermore, PB-modified $Fe_3O_4$ nanoparticles have been immobilized on the surface of glassy carbon electrode and applied to construct a sensor, it showed two well-defined pairs of redox peaks and a dramatic catalysis for the reduction of $H_2O_2$, which might be exploited to develop a new type of biosensor without any mediator.

## Introduction

Recently, nanosized magnetic materials have gained increasing interest for their novel properties, which could have promising applications in various technologies.[1]

Among these materials, magnetite ($Fe_3O_4$) is one of the most commonly studied superparamagnetic nanoparticles. For the unique mesoscopic physical and mechanical properties, it offers a lot of potential applications in several fields such as information storage,[2] color imaging,[3] microwave absorption,[4] medical diagnosis,[5] cell separation,[6] and so on. However, pure magnetic particles themselves may not be very useful in practical applications because of the following limitations: first, compared to other nanoparticles, they are more likely to aggregate for their large ratio of surface area to volume and strong magnetic dipole−dipole attractions between particles; second, their original structure may be changed if they are not sufficiently stable and result in the alteration of magnetic properties; and third, they can undergo rapid biodegradation when they are directly exposed to the biological system. Therefore, one of the main problems in the research of superparamagnetic nanoparticles is to modify the surface during the synthesis or coating process to overcome such limitations.

$Fe_3O_4$ has been modified with many kinds of polymers,[7] semiconductor material,[8] and metal.[9] In general, surface modification can be accomplished by physical and/or chemical adsorption or surface coating of desired molecules, depending on the specific applications. A silica coating on the surface of nanosized iron oxide particles, for example, could help prevent their aggregation in liquids and improve their chemical stability.[10] And starch-coated $Fe_3O_4$ nanoparticles showed the possibility of being transported in the extracellular space.[11] Many polymers such as polystyrene-poly (3-vinylpyridine),[12] poly(pyrrole),[13] and poly(vinyl alcohol),[14] as well as natural polymers such as dextran[15] and

* To whom correspondence should be addressed. E-mail: hychen@nju.edu.cn.

(1) Beecroft, L. L.; Ober, C. K. *Chem. Mater.* **1997**, *9*, 1302.
(2) Chakraborty, A. *J. Magn. Magn. Mater.* **1999**, *204*, 57.
(3) Ziolo, R. F. U. S. Patent 4,474,866, 1984.
(4) Pinho, M. S.; Gregori, M. L.; Nunes R. C. R.; Soares, B. G. *Polym. Degrad. Stab.* **2001**, *73*, 1.
(5) Josephson, L.; Tung, C. H.; Moore, A.; Weissleder, R. *Bioconj. Chem.* **1999**, *10*, 186.
(6) Sieben, S.; Bergemann, C.; Lubbe, A.; Brockmann, B.; Rescheleit, D. *J. Magn. Magn. Mater.* **2001**, *225*, 175.
(7) (a) Lin, H.; Watanabe, Y.; Kimura, M.; Hanabusa, K.; Shirai, H. *J. Appli. Polym. Sci.* **2003**, *87*, 1239. (b) Deng, J. G.; He, C. L.; Peng, Y. X.; Wang, J. H.; Long, X. P.; Li, P.; Chan S. C. Albert. *Synth. Met.* **2003**, *139*, 295. (c) Matsuno, R.; Yamamoto, K.; Otsuka, H.; Takahara, A. *Chem. Mater.* **2003**, *15*, 3.
(8) (a) Santra, S.; Tapec, R.; Theodoropoulou, N.; Dobson, J.; Hebard, A.; Tan, W. H. *Langmuir* **2001**, *17*, 2900. (b) Beydoun, D.; Amal. R.; Low, G. K. C.; McEvoy, S. *J. Phys. Chem. B* **2000**, *104*, 4387.
(9) Mikhaylova, M.; Kim, D. K.; Bobrysheva, N.; Osmolowsky, M.; Semenov, V.; Tsakalakos, T.; Muhammed, M. *Langmuir* **2004**, *20*, 2472.
(10) Zhu, Y. H.; Da, H.; Yang, X. L.; Hu, Y. *Colloids Surf. A* **2003**, *231*, 123.
(11) Kim, D. K.; Mikhaylova, M.; Wang, F. H.; Kehr, J.; Bjelke, B.; Zhang, Y.; Tsakalakos, T.; Muhammed, M. *Chem. Mater.* **2003**, *15*, 4343.
(12) Matsuno, R.; Yamamoto, K.; Otsuka, H.; Takahara, A. *Macromolecules* **2004**, *37*, 2203.
(13) Suri, K.; Annapoorni, S.; Tandon, R. P.; Mehra, N. C. *Synth. Met.* **2002**, *126*, 137.
(14) Lee, J.; Isobe, T.; Senna, M. *J. Collid. Interface Sci.* **1996**, *177*, 490.

10.1021/cm048078s CCC: $30.25 
Published on Web 05/13/2005

chitosan[16] have been used for modifying the surface of magnetic particles to achieve desirable surface functionalities.

However, to our knowledge, the synthesis of magnetite modified with coordination polymers has not been reported. It is well known that these kinds of complexes have many applications in catalysis, gas adsorption, and ion exchange. So if the advantages of coordination polymers and magnetite are combined, the potential applications of these complexes might be greatly widened. Prussian Blue (PB), which can be indexed as $M_i^{m+}$ $[M'(CN)_6]^{n-}$, has played a lot of important roles in the fields of magnetic molecules,[17] electrochromic devices,[18] and rechargeable batteries[19] for its interesting electrochemical, photophysical, and magnetic properties. Especially in the field of electroanalytical chemistry, it attracts the attention of the biosensor community.[20] Because of its analogy with the biological family of peroxidase, responsible in nature for the reduction of hydrogen peroxide,[21] it has been defined as an artificial peroxidase in the literature[22] and effectively catalyses the reduction of $H_2O_2$. Additionally, for its good electrochemical behavior, it can be used as a mediator in many biosensor systems to accelerate the electron transfer between the electrode and the enzymes.[23]

$Fe_3O_4$, for its good biocompatibility, strong superparamagnetism, low toxicity, and easy preparation process, has just begun to be used in biosensors and showed an attractive prospect.[24] Just recently, a series of about 1 $\mu$m dimensional magnetite particles functionalized with electroactive species such as ferrocene derivatives[25] and quinones complexes[26] were synthesized and then bonded to enzyme or DNA; with the external magnetic field as a triggering signal, the electrochemical catalytic properties of electroactive species toward the substrate changed greatly, which can be used as DNA sensing[27] or biochemiluminescence switch. However, the synthesis process is relatively complicated, and the influences of modifier on the magnetic properties of $Fe_3O_4$ and particle interactions have not been investigated.

As mentioned above, the disadvantages of $Fe_3O_4$ nanoparticles limit its many applications, so new coating is needed; it can not only prevent it from aggregating but more importantly can exploit its applications to other fields. We imagined that when modified with PB, based on the excellent electrochemical behavior and catalytic property of PB and on the good biocompatibility of $Fe_3O_4$, the resultant nanoparticles might be used to construct a kind of biosensor in which mediators or peroxidase are not necessary and the fabrication of the biosensors could be greatly simplified. Also the magnetic properties of samples might be affected in the presence of PB. In this paper, we presented a simple approach to synthesize PB modified $Fe_3O_4$ (simplified as PB−$Fe_3O_4$) nanoparticles and tried preliminarily to apply to the fabrication of the sensors. The electrical and magnetic properties of the composite were discussed in detail based on the structural characterizations including transmission electron microscopy (TEM), Fourier-transform IR (FTIR), UV, X-ray powder diffraction (XRD), X-ray photoelectron spectroscopy (XPS), and the influence of PB on $Fe_3O_4$ were also investigated by measuring its magnetic properties as a function of the temperature and an external magnetic field. As expected, the blocking temperature of PB−$Fe_3O_4$ decreased in comparison with that of pure $Fe_3O_4$, indicating the decrease of the interaction between the particles. We immobilized this material onto the surface of the glassy carbon electrode and found that a PB−$Fe_3O_4$-modified electrode shows a typical electrochemical behavior of PB and catalyses the reduction of $H_2O_2$, which displays a potential application of magnetite to electrocatalysis.

## Experimental Section

**Chemicals and Materials.** All chemicals were of reagent grade and used without further purification. Ferric(III) chloride, ferrous(II) sulfate, potassium ferricyanide, and sodium hydroxide were purchased from Shanghai Jinshan Chemical Company. Phosphate buffer solutions (PBS, 0.025 mol/L) with various pH values were prepared by mixing stock standard solutions of $K_2HPO_4$ and $KH_2PO_4$ and adjusted the pH with $H_3PO_4$ or NaOH.

Distilled deionized water was used for the preparation of all aqueous solutions. $N_2$ gas was passed through the solution to avoid possible oxygen action during the main synthesis steps.

**Preparation of $Fe_3O_4$ and PB−$Fe_3O_4$ Nanoparticles.** The $Fe_3O_4$ nanoparticles were prepared by the coprecipitation method according to the literature.[28] Briefly, 5.0 mL of iron ion solution containing 0.10 mol/L $Fe^{2+}$ and 0.20 mol/L $Fe^{3+}$ was added dropwise into 50 mL of alkaline solution (2 mol/L NaOH) under vigorous mechanical stirring for 30 min at 80 °C. The precipitated product was collected and removed from the solution by applying an external magnetic field and was washed with water until the supernatant solution turned neutral.

PB−$Fe_3O_4$ nanoparticles were prepared as follows: $Fe_3O_4$ nanoparticles were suspended in 10 mL of a solution of 0.10 mol/L $K_3[Fe(CN)_6]$ containing 10 mmol/L HCl and stirred for about 30 min, then a further 10 mL of 0.10 mol/L $FeCl_3$ solution containing 10 mmol/L HCl was added, and the resultant mixture was stirred for 30 min. The obtained particles were then collected by magnet and washed with 10 mmol/L HCl until the washing solution became colorless and then dried in a vacuum at room temperature.

**Preparation of PB−$Fe_3O_4$-Modified Glassy Carbon Electrodes.** The glassy carbon electrodes (GCE, 3 mm in diameter) were polished with 1.0, 0.3, and 0.05 $\mu$m alumina slurry (Beuhler)

(15) Molday, R. S.; Mackenzie, D. *J. Immunol. Methods* **1982**, *52*, 353.
(16) An, X.; Su, Z. J. *Appl. Polym. Sci.* **2001**, *81*, 1175.
(17) Buschmann, W. E.; Ensling, J.; Gutlich, P.; Miller, J. S. *Chem.−Eur. J.* **1999**, *5*, 3019.
(18) Mortimer, R. J.; Warren, C. P. *J. Electroanal. Chem.* **1999**, *460*, 263.
(19) Honda, K.; Hayashi, H. *J. Electrochem. Soc.* **1987**, *134*, 1330.
(20) (a) Ricci, F.; Amine, A.; Palleschi, G.; Moscone, D. *Biosen. Bioelectron.* **2003**, *18*, 165. (b) Raitman, O. A.; Katz, E.; Willner, I.; Chegel, V. I.; Popova, G. V. *Angew. Chem., Int. Ed.* **2001**, *40*, 3649.
(21) Gorton, L. *Electroanalysis* **1995**, *7*, 23.
(22) Karyakin, A. A.; Karyakina, E. E.; Gorton, L. *Anal. Chem.* **2000**, *72*, 1720.
(23) Li, J. P.; Peng, T. Z.; Peng. Y. Q. *Electroanalysis* **2003**, *15*, 1031.
(24) (a) Yang, H. H.; Zhang, S. Q.; Chen, X. L.; Zhuang, Z. X.; Xu, J. G.; Wang. X. R. *Anal. Chem.* **2004**, *76*, 1316. (b) Cao, D. F.; He, P. L.; Hu, N. F. *Analyst* **2003**, *128*, 1268. (c) Li, J. S.; He, X. X.; Wu, Z. Y.; Wang, K. M.; Shen, G. L.; Yu, R. Q. *Anal. Chim. Acta* **2003**, *481*, 191.
(25) Hirsch, R.; Katz, E.; Willner, I. *J. Am. Chem. Soc.* **2000**, *122*, 12053.
(26) Katz, E.; Sheeney-Haj-Ichia, L.; Buckmann, A. F. Willner, I. *Angew. Chem., Int. Ed.* **2002**, *41*, 1343.
(27) (a) Patolsky, F.; Weizmann, Y.; Katz, E.; Willner I. *Angew. Chem., Int. Ed.* **2003**, *42*, 2372. (b) Weizmann, Y.; Patolsky, F.; Katz, E.; Willner I. *J. Am. Chem. Soc.* **2003**, *125*, 3452.
(28) Kim, D. K.; Mikhaylova, M.; Zhang, Y.; Muhammed, M. *Chem. Mater.* **2003**, *15*, 1617.

followed by rinsing thoroughly with doubly distilled water and then allowed to dry at room temperature.

PB−$Fe_3O_4$ nanoparticles were dispersed in water to form a 1 mg/mL solution and ultrasonicated for 30 min, 8 $\mu$L of colloidal solution was dropped on the pretreated GCE surface and allowed to dry under ambient conditions for 3 h.

**Characterization.** The TEM micrographs were recorded using a JEOL 2000CX transmission electron microscope. A drop of the prepared nanosized magnetic particle suspensions was placed on carbon-coated copper grids and dried under ambient conditions.

UV−vis absorbance spectroscopy was performed using a UV-2201 spectrophotometer (Shimadzu, Kyoto, Japan). FTIR spectra were obtained on a NEXUS 670 (Nicolet).

The structure of the precipitated product was obtained by XRD with a Philips PW 1830 diffractometer, using a monochromatized X-ray beam with nickel-filtered Cu K$\alpha$ radiation.

XPS measurements were performed with an Ultra Axis spectrometer (Kratos Analytical Ldt., Manchester, UK) equipped with a monochromatic Al K$\alpha$ source operated at 150 W.

The DC magnetic properties of the samples were measured using a 7-T Quantum Design superconducting quantum interference device (SQUID) magnetometer. The zero-field cooled (ZFC) and field-cooled (FC) measurements were performed by cooling the sample to 5 K at zero field or in the presence of an external field of 100 Oe, respectively. All the magnetic measurements during the warming runs were carried out in a field of 100 Oe. AC magnetic measurements were also performed; the driving field was 100 Oe, while the frequency was varied from 1 to 100 Hz.

Electrochemical experiments were conducted with an Autolab PGSTAT 30 System (Ecochemie, The Netherlands) in a three-electrode system. All electrochemical experiments were carried out in a cell containing 10.0 mL of 0.025 mol/L PBS at room temperature (20 ± 2 °C) and using a platinum wire as auxiliary, a saturated calomel electrode as reference, and the PB−$Fe_3O_4$-modified electrode as a working electrode.

## Results and Discussion

TEM images show that, before modification, the morphology of $Fe_3O_4$ is somewhat irregularly shaped from oval to sphere, the verge of the nanoparticles is not very clear due to the interaction between particles, and the average size is about 8 nm. The particles tend to be larger and the size is about 12 nm after modification with PB (see Supporting Information).

Since there is a large ratio of surface to volume, high surface activity, and a high amount of dangling bonds on the nanoparticles' surfaces, the atoms on the surface are apt to adsorb ions. $Fe_3O_4$ easily adsorbs lattice ion $Fe^{3+}$ in the process of co-precipitation, and further $Fe(CN)_6^{3-}$ could be adsorbed; on the other hand, the isoelectric point of $Fe_3O_4$ is about 6.5,[29] in diluted HCl solution, the surface charge is positive, and $Fe(CN)_6^{3-}$ can be attracted on the surface of $Fe_3O_4$ for the static electric interactions. Both of the two factors promote the adsorption of $Fe(CN)_6^{3-}$; further adsorption of $Fe^{3+}$ will result in the form of PB. The fact was confirmed by the FTIR spectra of PB−$Fe_3O_4$.

Curve b in Figure 1 shows the FTIR absorption of PB−$Fe_3O_4$ compared to pure $Fe_3O_4$, bands at 2082 $cm^{-1}$ show the common characteristic of PB and its analogues, corresponding to the stretching vibration of the CN group,[30] and absorption bands at 499 $cm^{-1}$ are due to the formation of M−CN−M′,[31] which indicates the presence of PB. In addition, the absorption bands near 3415 and 1610 $cm^{-1}$ refer to the O−H stretching mode and H−O−H bending mode, respectively, indicating the presence of interstitial water in the samples.[32] It was previously reported that the characteristic absorption band of the Fe−O bond[33] was about 570 $cm^{-1}$. However, in Figure 1, the bands shift to a higher wavenumber of 602 $cm^{-1}$. A basic effect of finite size of nanoparticles is the breaking of a large number of bonds for surface atoms resulted in the rearrangement of unlocalized electrons on the particle surface. As a result, when particles were reduced to nanoscale dimensions, the absorption bands of FTIR spectra shift to higher wavenumber. So the red shift of absorption bands of the Fe−O bond can be observed.

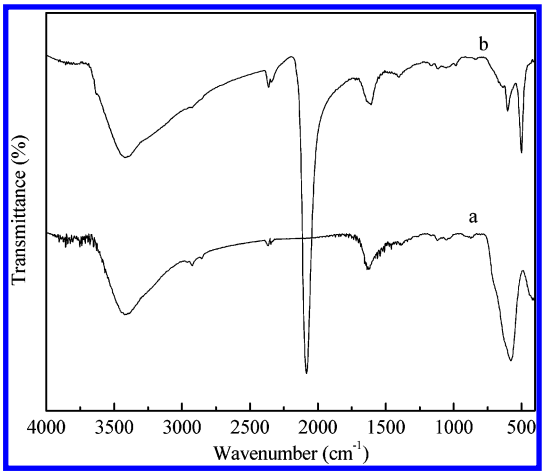


**Figure 1.** FTIR spectra of $Fe_3O_4$ nanoparticles before (a) and after (b) modification with PB.

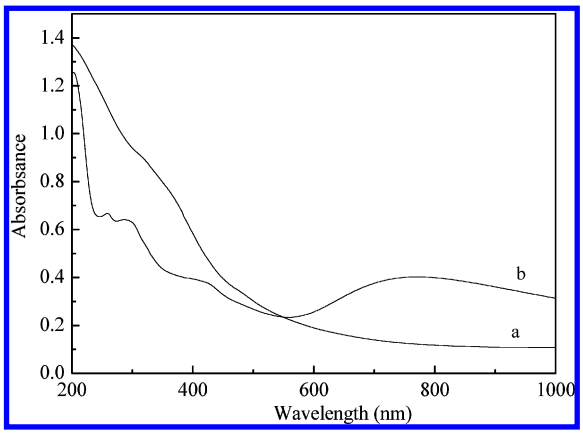


**Figure 2.** Absorption spectra of unmodified (a) and PB-modified (b) $Fe_3O_4$ nanoparticles.

Figure 2 shows the UV−vis absorption spectra of (a) unmodified and (b) PB-modified $Fe_3O_4$ particles. In the case of unmodified magnetite particles, no obvious absorbance could be found, while for PB−$Fe_3O_4$, the mixed-valence charge-transfer band of the polymeric [$Fe^{II}$−C−N−$Fe^{III}$] sequence at 780 nm can be observed, and the other bands

(29) Regazzoni, A. E.; Urrutia, G. A.; Blesa, M. A.; Maroto, A. J. G. *J. Inorg. Nucl. Chem.* **1981**, *43*, 1489.
(30) Ayers, J. B.; Piggs, W. H. *J. Inorg. Nucl. Chem.* **1971**, *33*, 721.
(31) Wilde, R. E.; Ghosh, S. N.; Marshall, B. J. *Inorg. Chem.* **1970**, *9*, 2512.
(32) Itaya, K.; Uchida, I.; Neff, V. D. *Acc. Chem. Res.* **1986**, *19*, 162.
(33) Waldron, R. D. *Phys. Rev.* **1955**, *99*, 1727.

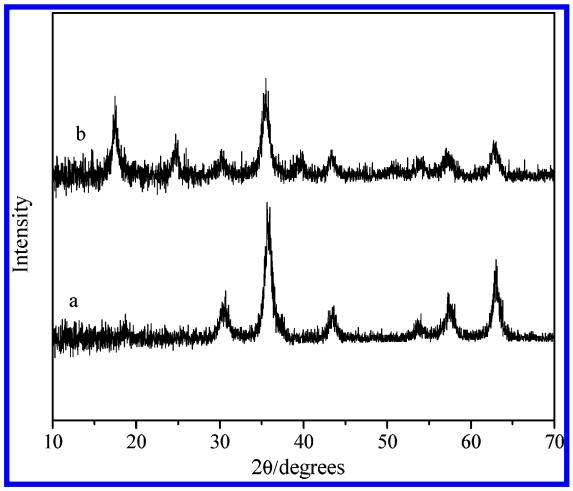


**Figure 3.** XRD patterns of pure (a) and PB-modified (b) $Fe_3O_4$ nanoparticles.

are also the characteristic absorption of PB, which is in accordance with the literature previously reported.[34]

XRD patterns of unmodified (a) and PB modified (b) $Fe_3O_4$ nanoparticles are shown in Figure 3. The diffractograms of the two sample peaks correspond to the spinel structure. According to the literature, the samples prepared by a co-precipitation process can be expected as magnetite with a pure phase on the basis of the results from thermodynamic modeling.[35] In the case of PB−$Fe_3O_4$, the characteristic peaks of PB cubic space group[36] ($2\theta$ = 17.6, 24.8, and 39.6°) are also observed, which further confirmed the existence of PB in the sample.

XPS was also used to characterize the samples in a wide scan. In the spectrum of PB−$Fe_3O_4$ nanoparticles, compared to that of pure $Fe_3O_4$, a new peak at 398 eV is observed, which is the position of N1s, indicating the presence of −CN (see Supporting Information).

In this paper, we have studied the magnetic properties of PB−$Fe_3O_4$ nanoparticles in detail. The temperature dependence of magnetization of the PB−$Fe_3O_4$ nanoparticles (Figure 4) at 100 Oe after ZFC and subsequent FC at 100 Oe are not reversible, and a point of intersection at about 150 K was observed. It corresponds to the blocking temperature ($T_B$), which is lower than that of the pure $Fe_3O_4$ (220 K). Without PB modification, for the increase in the large ratio of surface area to volume, the attractive force between nanoparticles will increase, leading to the aggregation of the nanoparticles. These agglomerated nanoparticles may act as a cluster, resulted in an increase of $T_B$. In contrast, the PB−$Fe_3O_4$ nanoparticles are more freely aligned with the external field than the unmodified nanoparticles and behave independently; the interactions between each other are therefore not important. Below 12 K in Figure 4, a ferromagnetic-like phenomenon was observed in PB− $Fe_3O_4$ nanoparticles; we suggest the superferromagneic behavior in it.[37]

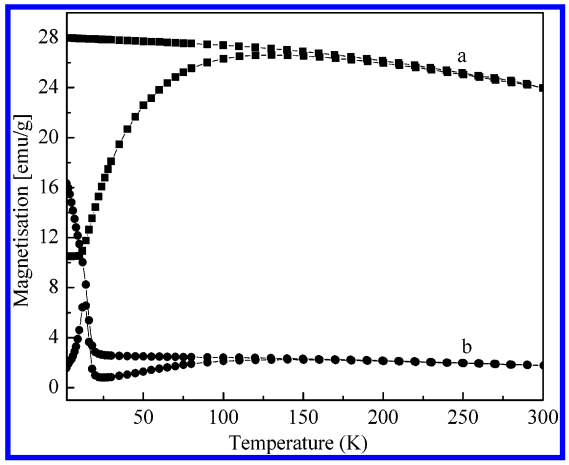


**Figure 4.** ZFC at 100 Oe and FC measurements of pure $Fe_3O_4$ (a) and PB-modified $Fe_3O_4$ nanoparticles (b).

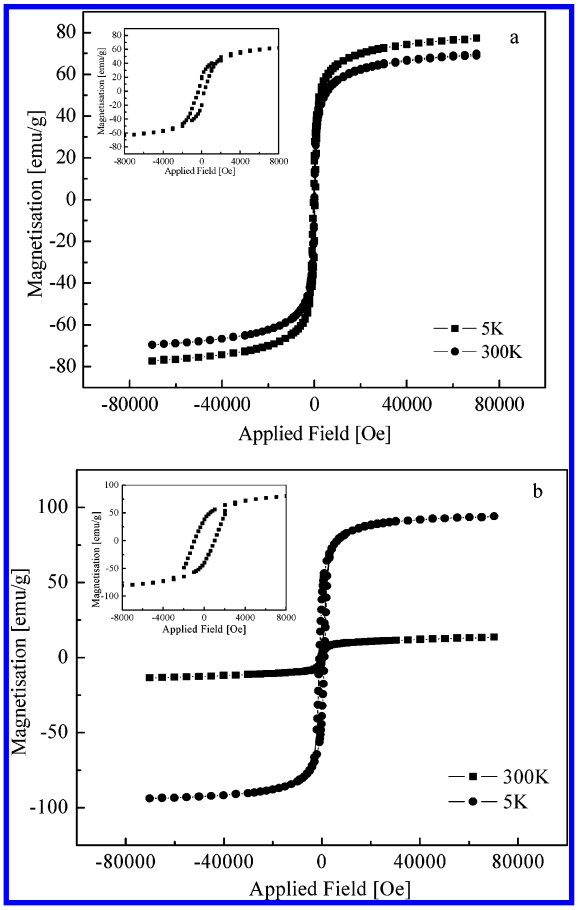


**Figure 5.** Magnetization measurements as a function of applied magnetic field for (a) pure $Fe_3O_4$ and (b) PB-modified $Fe_3O_4$ nanoparticles at 5 and 300 K. The insets are the magnetization measurements at 5 K.

The saturation magnetization (Ms), coercivity, and remanence magnetization are derived from the SQUID measurements for the PB-modified and unmodified $Fe_3O_4$ at 5 and 300 K (Figure 5). The typical superparamagnetic behaviors are observed by showing almost immeasurable coercivity and remanence above the $T_B$ (at 300 K), which is also the characteristic property for magnetite. When temperature is below the $T_B$ (at 5 K), both of the samples showed a slight magnetic hysteresis. For pure $Fe_3O_4$, the Ms is almost the same at 5 and 300 K, 70 emu/g, which is just less than that of the bulk magnetite (92 emu/g).[38] The difference in magnetization value between bulk and our nanoparticles

(34) Pyrasch, M.; Tieke, B. *Langmuir* **2001**, *17*, 7706.
(35) Kim, D. K.; Zhang, Y.; Voit, W.; Rao, K. V.; Kehr, J.; Bjelk, B.; Muhammed, M. *Scr. Mater.* **2001**, *44*, 1713.
(36) Buuser, H. J.; Schwarzenbach, D.; Petter, W.; Ludi, A. *Inorg. Chem.* **1977**, *16*, 2704.
(37) Li, G. D. *Today Magnetism*; Science Press: Bejing, 1999; p 18.

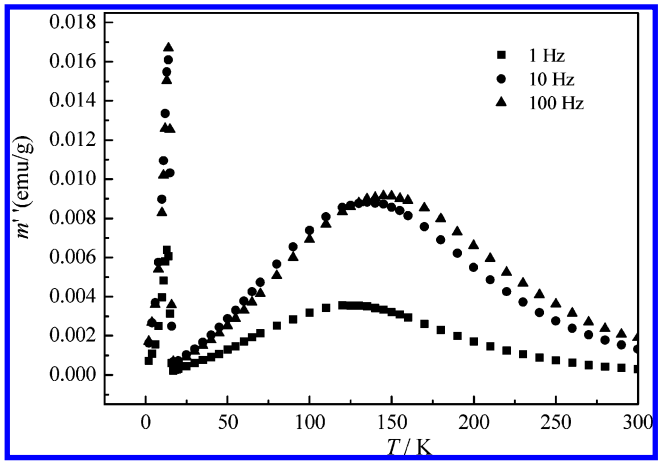


**Figure 6.** AC magnetic susceptibility data for PB−$Fe_3O_4$ nanoparticles in the frequency range of 1−100 Hz.

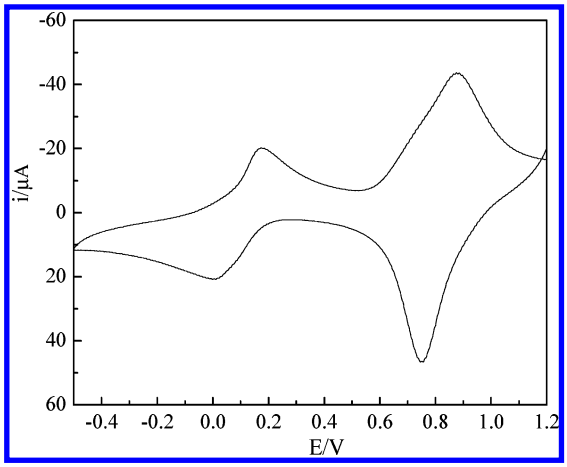


**Figure 7.** Cyclic voltammogram of the PB−$Fe_3O_4$-modified GCE in pH 6.0 PBS, scan rate 100 mV/s.

might be attributed to the small particle size effect. For PB−$Fe_3O_4$, the Ms at 300 K is 12 emu/g, the decrease may be ascribed to the presence of the PB layer on the surface of $Fe_3O_4$. However, at 5 K, Ms increased greatly to 80 emu/g, just like mentioned above, the ferromagnetic behavior of PB−$Fe_3O_4$ below 12 K resulted in this phenomenon. Also this will explain the difference between the loops of the two samples.

The dynamics of magnetic relaxation were investigated using alternating current (AC) magnetic susceptometry (Figure 6). The cusp temperature, i.e., the temperature corresponding to the maximum of the in-phase component of the AC susceptibility, corresponds to the $T_B$. There are two maximum points at the two curves. With the change of the frequency, the maximum point about 150 K changed accordingly, which is also the characteristic of superparamagnetic nanoparticles, the maximum point at 12 K almost unchanged, this is due to the ferromagnetic behavior, which is the same as discussed above. For a noninteracting single particle with barrier energy $E_0$ and uniaxial anisotropy fluctuations, the thermal relaxation process follows the Néel−Arrhenius law,[39] $\tau_r = (1/f_0) \exp(E_0/k_BT)$, where $\tau_r$ is the relaxation time of the magnetic moment of the particle, $f_0$ is the attempt frequency of the transition, $k_B$ is the Boltzmann constant, and $T$ is the absolute temperature. $E_0$ and $f_0$ can be directly obtained by AC magnetic susceptometry measurements. At $T_B$, $\tau_r$ is equal to the time scale of the measurement and can be expressed by $\tau_m = 1/f_0$. The plot of $-\ln(f_0)$ vs $1/T_B$ gives a linear curve, the slope corresponds to $E_0$, and the intercept is $\tau_m$. The exponential factor $\tau_m$ is usually found to be in the range of $10^{-9}$−$10^{-11}$ s for ferro- and ferrimagnetic nanoparticles. Our sample shows that the $\tau_r$ value follows the Néel−Arrhenius law but with an unphysical value of $1.6 \times 10^{-13}$ s. The obtained value is related to the interaction between nanoparticles as the change in the nanoparticle surface area influences the anisotropy energy barrier.

It is well known that PB bears good electrochemical behaviors and has been widely applied to the field of

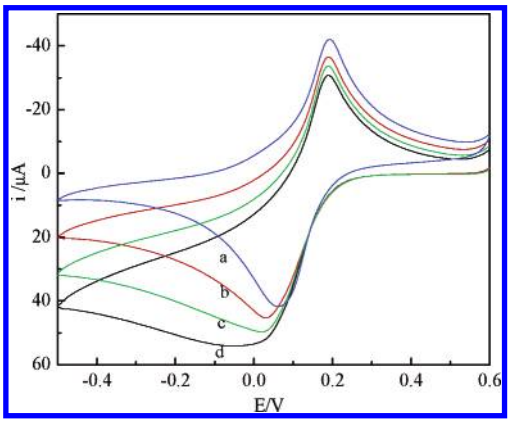


**Figure 8.** Cyclic voltammograms of PB−$Fe_3O_4$-modified nanoparticles electrode in the absence (a) and presence of 0.48 mmol/L (b), 0.96 mmol/L (c), and 1.44 mmol/L $H_2O_2$ (d) in pH 6.0 PBS, scan rate 100 mV/s.

chemically modified electrode. Here we tried to immobilize PB−$Fe_3O_4$ nanoparticles onto the surface of glassy carbon electrode and took it as an example to observe the new possible application of magnetic material in the third-generation biosensor without any mediator. It was reported that an autoreduction or a catalytic reduction of the highly reactive ferri−ferricyanide complex, which presumably is initially formed, seems to occur and form the PB.[40] Electrochemical behaviors of PB−$Fe_3O_4$-modified electrode can confirm this. In pH 6.0 PBS (Figure 7), the two typical pairs of redox waves showing the oxidation of Prussian Blue to Prussian Green as well as the reduction to Prussian White were observed for the PB−$Fe_3O_4$-modified GCE, indicating the effective presence of PB in the sample.

The effect of the potential scan rate ($\nu$) on the peak current ($ip_a$ and $ip_c$) has been investigated in the range of 10−100 mV/s; the results showed that the relationship between peak current and the square root of the scan rate ($\nu^{1/2}$) for the redox reaction between Prussian Blue and Prussian White is linear. Obviously, from the shape of voltammogram, the electrode processes are rate determining.[41]

The influence of PBS pH values on the electrochemical behavior of PB−$Fe_3O_4$-modified electrode was also studied.

(38) Zaitsev, V. S.; Filimonov, D. S.; Presnyakov, I. A.; Gambino, R. J.; Chu, B. *J. Colloid Interface Sci.* **1999**, *212*, 49.
(39) Néel, L. A. *Geophys.* **1949**, *5*, 11.
(40) Itaya, K.; Akahoshi, H.; Toshima, S. *J. Electrochem. Soc.* **1982**, *129*, 1498.
(41) Zakharchuk, N. F.; Meyer, B.; Hennig, H.; Scholz, F.; Jaworsi. A.; Stojek, Z. *J. Electroanal. Chem.* **1995**, *398*, 23.

With the increasing pH value from 3.0 to 8.0, the redox peak potential almost unchanged, it revealed that no proton is involved in the electrochemical reaction of PB, but the peak current gradually decreased, since PB is not very stable in neutral and alkaline solution, and Prussian White is somewhat solvable in water.

In the potential range of 0.6 and −0.5 V, the cyclic voltammograms of modified electrode in PBS before and after the addition of $H_2O_2$ were shown in Figure 8. It can be seen that with the gradual addition of $H_2O_2$, the reduction peak current for PB increased and the oxidation peak current decreased gradually, which showed the catalytic properties of modified electrode to the reduction of $H_2O_2$.

## Conclusions

Electroactive PB-modified $Fe_3O_4$ nanoparticles can be prepared by a simple chemical method. The obtained product retained the superparamagnetic properties, while the blocking temperature decreased compared to that of the pure $Fe_3O_4$ nanoparticles, so the dipole−dipole interactions between the magnetic particles decreased, which will decrease the rate of aggregation of nanoparticles and prolong their life span. Furthermore, this kind of material could be applied to the chemical modified electrode and effectively catalyses the reduction of $H_2O_2$, which shows a new applicable prospect for $Fe_3O_4$ in fabricating a new kind of biosensor without mediator.

**Acknowledgment.** This project was supported by the National Natural Science Foundation of China (Nos. 90206037 and 20475025) and Science Foundation of Jiangsu (No. BK 2004210).

**Supporting Information Available:** TEM images and XPS spectra. This material is available free of charge via the Internet at http://pubs.acs.org.

CM048078S